Supplementary information for:

First Principles Study of Tetracene under Pressure

Mayami Abdulla [1], Keith Refson [2,3], Richard H. Friend [1], Peter D. Haynes [4]

[1] Department of Physics, University of Cambridge, Cavendish Laboratory, 19 J. J. Thomson Avenue, Cambridge CB3 0HE, UK

[2] ISIS Facility, STFC Rutherford Appleton Laboratory, Chilton, Didcot, Oxfordshire OX11 0QX, UK

[3] Department of Physics, Royal Holloway, University of London, Egham, Surrey TW20 0EX

[4] Departments of Materials and Physics, Imperial College London, Exhibition Road, London SW7 2AZ, UK

Optimised Structure

The x-ray structure of crystalline tetracene named TETCEN01.cif available in the Cambridge crystallography database (CCD) [1] is optimised using DFT-LDA. The results of unconstrained geometry optimisation are available in files (TETCEN01-LT175K-atm.cif) and (TETCEN01-LT175K-P280.cif) for tetracene crystal under ambient and 280MPa pressures, respectively.

Phonon Frequencies

Phonon dispersion curves were calculated along a path traversing the high symmetry points of the BZ defined in [2, 3] and a few points in between. The path along $\overline{\Gamma B}\left(\overline{KF}\right)$ and $\overline{BK}\left(\overline{F\Gamma},\overline{GZ}\right)$ involves **q**-point sampling in the reciprocal space along ***a****** and ***b****** axes while the path $\overline{\Gamma G}\left(\overline{ZF}\right)$ is along the ***c****** axis. The path along $\overline{\Gamma K}$ represents the sampling between the molecules positioned as edge-to-face within the ***ab****** plane.

Table S1 presents some of the theoretically DFT-LDA calculated phonon frequencies for tetracene at the centre of the BZ with a contrast with those experimentally measured in reference [4]. A complete result of phonons frequencies calculated using DFT-LDA for the optimised structure at ambient pressure, as well as the optimised compressed structure, is available in the files (Phonons_atm.xyz) and (Phonons_280MPa.xyz). The files contain information that can be utilised to view the displacement of atoms associated with each phonon mode.

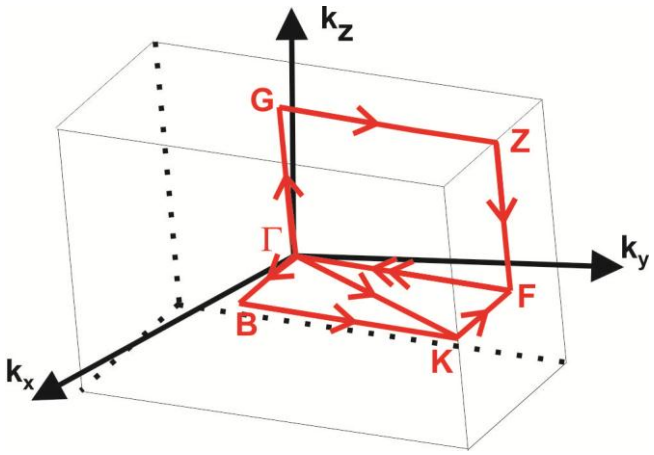

Figure S1. The Brillouin zone of the tetracene triclinic crystal. The high symmetry points are labelled as follows: $\Gamma = (0,0,0)$ $B = \left(\frac{1}{2}, 0, 0\right)$, $F = \left(0, \frac{1}{2}, 0\right)$, $G = \left(0, 0, \frac{1}{2}\right)$, $Z = \left(0, \frac{1}{2}, \frac{1}{2}\right)$ and $K = \left(\frac{1}{2}, \frac{1}{2}, 0\right)$.

Table S1. Theoretically DFT-LDA calculated phonon frequencies for tetracene at the centre of the BZ and those experimentally reported in reference Pivovar *et al*. [4]. The displacement direction is described as parallel (∥) or perpendicular (⊥) relative to the molecular plane.

DFT-LDA (This work)			Reference Pivovar et al. [4]			
calc.		Atomic	expt.		calc.	Atomic
1 atm	280MPa	displacement	1 atm	299MPa	(1 atm)	displacement
			29.6			
41.6	42.5	∥ & ⊥	47.2			
53.8	56.9	∥ & ⊥			56.72	⊥
61.4	65.3	∥ & ⊥				
73.2	75.9	⊥				
74.4	77.6	⊥				
80.4	84.2	∥				
101.6	110.6	⊥	90.4			
					92.24	⊥
115.9	122.9	⊥				
117.5	126.1	⊥				
132.1	140.8	⊥	132.8			
146.7	154.1	⊥				
147	157.2	⊥				
157.4	163.5	⊥	167.2		151.76	⊥
169.2	171.1	∥			162.88	∥
174.8	179.7	⊥				
177.3	181.9	⊥				
178	182.4	⊥				
218.7	223.6	⊥	212.8	218.4	195.2	⊥
223.8	229.5	⊥				
272	273.3	⊥	269.6	272	273.6	⊥
280	286.4	⊥				
302.9	303.6	∥	300	300	303.2	∥
305.8	306.6	∥				
318.4	319.1	∥	320.8	324.8	318.4	∥ & ⊥
325.2	326.9	∥				
329.1	331.9	⊥			321.6	⊥
332.3	335.5	⊥				
389.8	391.6	⊥	377.6	378.4	383.2	⊥
395	397.8	⊥				
436.7	436.6	∥	435.2	434.4	444.8	∥
438.4	438.5	∥				
460.2	460.9	⊥				
471.5	472.4	⊥				
476.1	478.6	⊥	472	473.6	479.2	⊥
483.1	484.2	⊥			481.6	⊥
485.2	487.8	⊥			487.2	⊥
491.5	493.9	⊥				
496.7	497.0	∥				
498.7	499.2	∥				
509.0	509.1	⊥	500		504.8	∥ & ⊥
516.6	517.5	⊥			520.8	⊥
553.9	554.9	∥	545.6	546.4	563.2	∥ & ⊥
557.5	557.9	∥				
569	569.8	⊥			568	∥ & ⊥

Debye Frequency and Temperature

Utilising the phonon dispersion information, the Debye frequency (ω_D) and temperature (Θ_D) at ambient pressure (280MPa) are computed to be 127.8cm^{-1} (149.1cm^{-1}) and 29.3K (34. 1K) respectively. These values are much lower than those exhibit by anthracene and naphthalene [5-7].

The Specific Heat Capacity of Tetracene Crystal

The heat capacity is the amount of heat required to raise the temperature of the sample by one degree whilst the heat capacity per unit mass, volume or one mole of the substance is the specific heat capacity c_v. The phonon frequencies computed at **q**-vectors of a fine MP grid contribute to the specific heat c_v which, within the harmonic approximation, is given as follows:

$$c_v = k_B \sum_{\mathbf{k}s} \left(\frac{\hbar\omega_s(\mathbf{k})}{2k_B T} \right)^2 \frac{1}{\sinh^2\left(\frac{\hbar\omega_s(\mathbf{k})}{2k_B T} \right)} \qquad \text{(S.1)}$$

Where ω_s is the frequency of the mode ***s***, $\hbar\omega_S$ – termed as vibrational excitation or phonon energy – corresponds to the mode ***s***, and k_B is Boltzmann. The summation is taken over the phonon modes computed at **q**-vectors of a fine MP grid over the entire BZ. Figure S2 shows the DFT-LDA calculated average specific heat capacity of tetracene at ambient pressure and 280MPa as a function of temperature. At temperatures well below the room temperature where $(\hbar\omega \rangle\rangle k_B T)$, the c_v will contain appreciable contribution from phonons, particularly acoustic phonons. The c_v increases as the temperature rises and eventually saturates to the classical limit stated by classical law of Dulong-Petit.

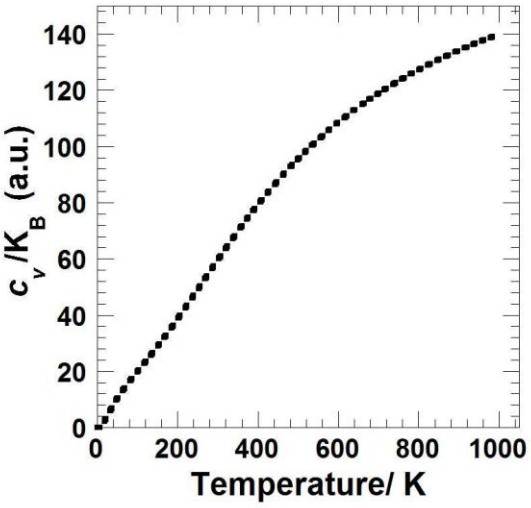

Figure S2. Theoretically DFT-LDA calculated averaged specific heat capacity c_v for tetracene as a function of temperature.

Grüneisen Parameter

The overall crystal Grüneisen parameter is determined by averaging over the individual Grüneisen parameter $\gamma_{\mathbf{k}s}$ of all the phonon modes with a weight of specific heat contribution $c_{vs}(\mathbf{k})$ from each mode as follows:

$$\gamma(T) = \frac{\sum_{\mathbf{k},s} \gamma_{\mathbf{k}s} c_{vs}(\mathbf{k})}{\sum_{\mathbf{k},s} c_{vs}(\mathbf{k})} \tag{S.2}$$

where $\gamma_{\mathbf{k}s}$ is the mode-specific Grüneisen parameter defined as:

$$\gamma_{\mathbf{k}s} = -\frac{\partial(\ln \omega_s(\mathbf{k}))}{\partial(\ln V)} = -\frac{V}{\omega_s(\mathbf{k})}\frac{\partial \omega_s(\mathbf{k})}{\partial V} \tag{S.3}$$

Figure S3 displays the crystal overall Grüneisen parameter calculated as a function of temperature. The figure shows the absence of negative values of Grüneisen parameter at high temperatures, indicating that tetracene does not exhibit negative thermal expansion defined by the decrease (increase) of mode frequencies when the volume decreases (increases) contrary to pentacene and anthracene [8, 9].

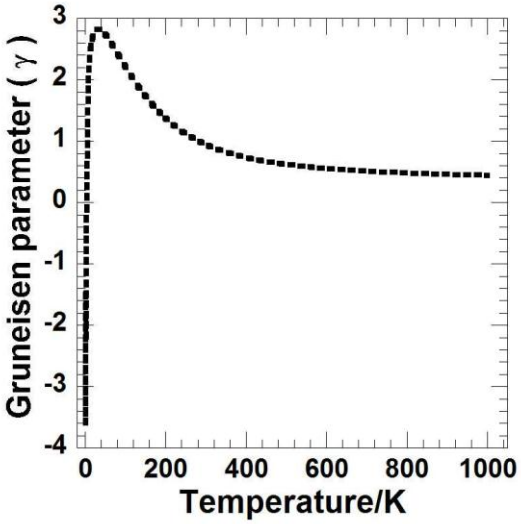

Figure S3. The DFT-LDA computed overall Grüneisen parameter of tetracene crystal as a function of temperature.

Pressure Dependence of Raman and infra red Spectra

Figure S4 presents the frequencies of the low-lying Raman-active modes at ambient pressure conditions calculated using DFT-LDA plotted against the experimentally measured frequencies in Ref.[10]. The results show excellent agreement, as indicated by the slope of (1.04±0.02) and correlation coefficient of 0.998. A small scaling error – in this case 1.04 is typical and expected of the comparison between DFT and experimental frequencies. There is clearly no deviation from the linear relationship between modes of intra- and intermolecular character, which supports our contention that the use of LDA to describe intermolecular interactions in molecular crystals still gives an excellent account of phonon frequencies despite its thermochemical failings.

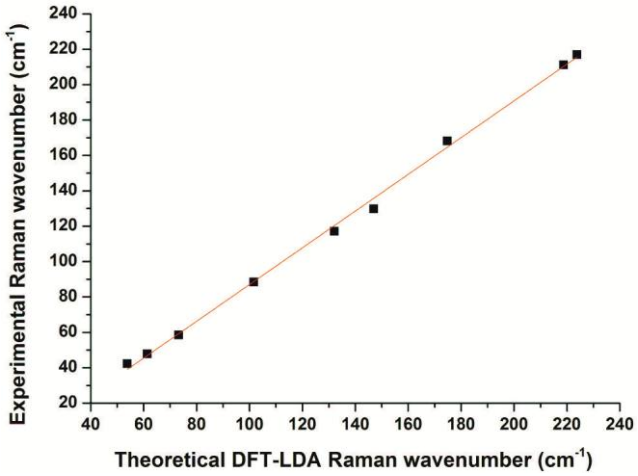

Figure S4. Correspondence between theoretically DFT-LDA calculated and experimentally measured Raman frequencies reported in reference [10] at ambient pressure condition for tetracene single crystals.

Quantitative comparison between frequencies of Raman modes calculated using DFT-LDA for tetracene unit cell and the frequencies reported in reference [10] is given in Table S2. The modes show a good overall agreement between DFT-LDA and the reported data except for some moderate inconsistencies at the very low frequencies.

The study presented here predicts a total of ten modes to be active in Raman spectra, which are all below 300 cm^{-1} – in contrast to reference [10] which theoretically predicts, using the *ab initio* calculation on an isolated molecule, the detection of the lowest intramolecular modes at 146.7 cm^{-1}. Table S3 reports the DFT-LDA calculated Raman frequencies for the intermolecular and intramolecular modes up to ~ 300 cm^{-1} at ambient and 280MPa pressures together with the mode-specific Grüneisen parameter. In general, the mode-specific Grüneisen parameter for the intermolecular modes below ~150 cm^{-1} exhibits large anharmonicity with a maximum value of $\gamma \approx 4.9$ demonstrated by the mode at 101 cm^{-1}, which corresponds to displacement of atoms perpendicular to the molecular plane. However, the intramolecular modes exhibit a very low mode Grüneisen parameter such that $\gamma < 1$ with a negligible change for some of the modes corresponding to atomic displacement parallel to the molecular plane.

Table S4 presents the modes' frequencies at ambient and 280MPa pressures and the associated mode-specific Grüneisen parameter with the assignment of the atomic displacements corresponding to the modes. Although the intermolecular infrared bands demonstrate very low intensity, the mode Grüneisen parameter is large compared to the intramolecular modes. The maximum mode Grüneisen parameter is ~4, exhibited by the mode 117 cm^{-1} which is associated with the displacement of atoms perpendicular to the molecular plane.

Table 2. The frequencies of the intermolecular and intramolecular Raman modes (in cm^{-1}) calculated using DFT-LDA and the previously reported results in reference [10].

DFT-LDA		Ref. [10]		
Ambient P	Displacement	expt.	calc.	*ab initio*
53.76	∥	42.3	36.5	-
61.38	∥ & ⊥	47.8	44.8	-
73.20	⊥	58.5	62.0	-
101.63	⊥	88.4	88.8	-
132.09	⊥	117.1	131.3	-
147.01	⊥	129.8	139.1	-
174.79	⊥	168.2	175.2	146.5
178.02	⊥		176.4	
218.73	⊥	211.2	221.1	188.2
223.84	⊥	217.0	225.3	

Table S3. The frequencies of the intermolecular and some of the intramolecular modes with the corresponding mode-specific Grüneisen parameter.

Ambient P (cm^{-1})	280MPa (cm^{-1})	γ per mode	displacement
53.76	56.92	3.23	∥
61.382	65.32	3.52	∥ & ⊥
73.20	77.58	3.29	⊥
101.63	110.62	4.86	⊥
132.09	140.82	3.63	⊥
147.01	157.24	3.83	⊥
174.79	179.71	1.55	⊥
178.02	182.38	1.35	⊥
218.73	223.60	1.22	⊥
223.84	229.53	1.40	⊥
302.93	303.63	0.13	∥

Table S4. The infrared intermolecular and some of the intramolecular modes with mode-specific Grüneisen parameter. The displacement direction is described as parallel (ıı) or perpendicular (⊥) relative to the molecular plane.

Ambient P	280MPa	γ per mode	displacement
41.62	42.50	1.16	ıı & ⊥
74.38	75.85	1.09	⊥
80.39	84.23	2.63	ıı
115.85	122.94	3.36	⊥
117.51	126.13	4.03	⊥
146.71	154.11	2.77	⊥
157.43	163.53	2.13	⊥
169.21	171.12	0.62	ıı
177.32	181.97	1.44	ıı & ⊥
272.42	273.28	0.17	⊥
280.31	282.63	0.46	⊥
329.08	331.90	0.47	⊥
332.32	335.55	0.53	⊥
436.72	436.63	-0.01	ıı
438.37	438.51	0.02	ıı
460.24	460.97	0.09	⊥
476.05	478.59	0.29	⊥
483.09	484.23	0.13	⊥
491.47	493.85	0.27	⊥
553.85	554.29	0.04	ıı
557.47	557.94	0.05	ıı
568.98	569.79	0.08	⊥
574.17	575.78	0.15	⊥
612.03	612.53	0.04	ıı
613.96	614.67	0.06	ıı

Pressure Dependence of Band Structure

The electronic dispersion curves for the LT tetracene structure at ambient and 280 MPa hydrostatic pressures are shown in Figure S5. Only the top of the valence band and the bottom of the conduction band close to the energy gap are displayed. The intermolecular interactions between the two inequivalent molecules in the unit cell cause the bands to split and appear in pairs such that the bands will have a finite width. The electronic states are singly degenerate except at some principal symmetry points. The DFT-LDA computed highest occupied molecular orbital (HOMO) is separated from the lowest unoccupied molecular orbital (LUMO) by a direct bandgap that is equal to 1.03 eV and is located at the principal symmetry point **K** (0.5,0.5,0). The arrangement of the molecules in the cell with their long axis approximately along the ***c**** direction leads to more intermolecular coupling in the ***ab**** plane and less along the ***c**** direction. Hence, the electronic dispersion curves display directional anisotropy so the transfer integral defined to be equal to half of the bandwidth is significantly anisotropic. This is indicated by the high electronic dispersion of the bands along the principal direction within the plane while it is almost negligible between the layers. Accordingly, there is hardly any dispersion along $\overline{G\Gamma}$ as revealed by the flat electronic bands. At ambient pressure, the band dispersion for HOMO and LUMO increases to a maximum along $\overline{BK}$ in a similar amount to that along the face-to-edge direction $\overline{\Gamma K}$. The associated coupling at **K** is 0.49 eV and 0.73 eV for the HOMO and LOMO, respectively. The transfer integrals corresponding to the HOMO and LOMO are 0.245 eV and 0.365 eV respectively.

The band gap is reduced after compressing the crystal, hence, the π-π coupling between molecules in the ***ab**** plane increases. This leads to enhancement of the electronic band splitting in the HOMO and LUMO to 0.515 eV and 0.75 eV respectively which corresponds to a transfer integral for the HOMO and LUMO of 0.258 eV and 0.38 eV, respectively. The increase of transfer integral results in an increase in the rate of charge transfer in the compressed tetracene relative to that at ambient pressure.

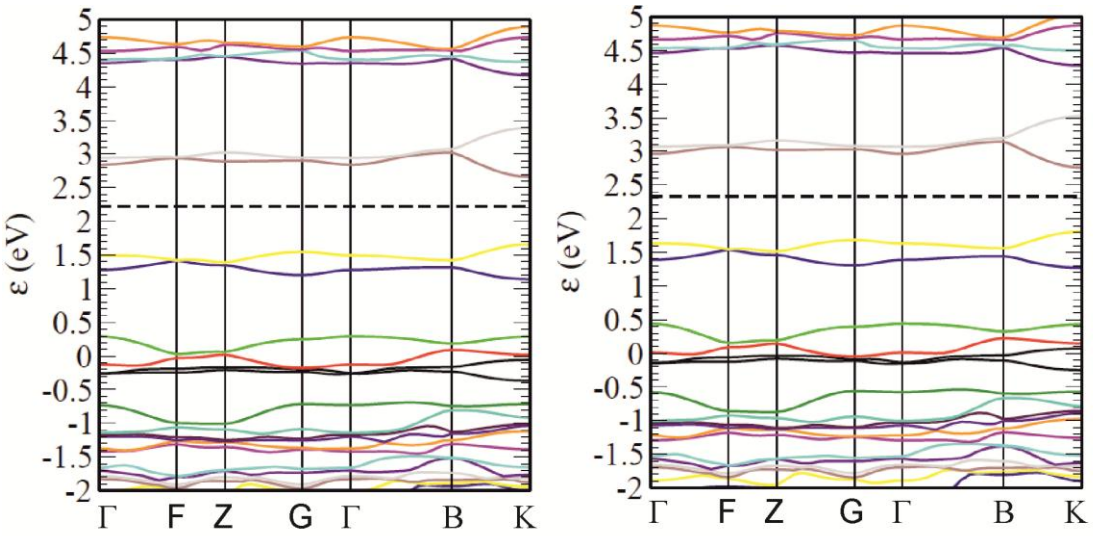

Figure S5. Theoretically DFT-LDA computed energy band structure of tetracene along the main directions of symmetry at ambient pressure (left) and 280MPa (right). The dashed line represents the Fermi level.

References

1. Holmes, D., et al., *On the nature of nonplanarity in the [N]Phenylenes.* Chemistry – A European Journal, 1999. **5**(11): p. 3399-3412.
2. Bradley, C.J. and A.P. Cracknell, *Mathematical theory of symmetry in solids: representation theory for point groups and space groups* 1972 Oxford: Oxford University Press.
3. Hummer, K. and C. Ambrosch-Draxl, *Electronic properties of oligoacenes from first principles.* Physical Review B, 2005. **72**(20): p. 205205.
4. Pivovar, A.M., et al., *Structural and vibrational characterization of the organic semiconductor tetracene as a function of pressure and temperature.* Chemical Physics, 2006. **325**(1): p. 138-151.
5. Munn, R.W. and G.S. Pawley, *Debye temperatures of anthracene.* physica status solidi (b), 1972. **50**(1): p. K11-K15.
6. Eggert, E. and H. Hänsel, *Characteristic Debye temperature of anthracene.* physica status solidi (b), 1971. **47**(1): p. K69-K73.
7. Sallamie, N. and J.M. Shaw, *Heat capacity prediction for polynuclear aromatic solids using vibration spectra.* Fluid Phase Equilibria, 2005. **237**(1-2): p. 100-110.
8. Haas, S., et al., *Large uniaxial negative thermal expansion in pentacene due to steric hindrance.* Physical Review B, 2007. **76**(20): p. 205203.
9. Fukuhara, M., A.H. Matsui, and M. Takeshima, *Low-temperature elastic anomalies in an anthracene single crystal.* Chemical Physics, 2000. **258**(1): p. 97-106.
10. Venuti, E., et al., *Phonons and structures of tetracene polymorphs at low temperature and high pressure.* Physical Review B, 2004. **70**(10): p. 104106.